Journal of Coordination Chemistry, 2013
Vol. 66, No. 16, 2875–2884, http://dx.doi.org/10.1080/00958972.2013.818139

Taylor & Francis
Taylor & Francis Group

Syntheses, crystal structures, and spectral characterization of an asymmetrically substituted 1,2,4-triazole and its iron(II) complex

JUN GONG, XIN HE, LANG CHEN, XUAN SHEN and DUNRU ZHU*

State Key Laboratory of Materials-oriented Chemical Engineering, College of Chemistry and Chemical Engineering, Nanjing University of Technology, Nanjing, P.R. China

(*Received 17 January 2013; in final form 15 May 2013*)

One new asymmetrically substituted 1,2,4-triazole, 4-amino-3-(*p*-bromophenyl)-5-(2-pyridyl)-1,2,4-triazole (**L**), and its iron(II) complex, *trans*-$[FeL_2(NCS)_2]$ (**1**), have been synthesized and characterized by elemental analyses, FT-IR, ^1H NMR, ESI mass spectra, and single-crystal X-ray crystallography. Crystallographic studies revealed that **1** contains a distorted octahedral $[FeN_6]$ core with two *trans* NCS^-. Each **L** adopts a chelating bidentate coordination via N of pyridyl and one N of the triazole ring. Magnetic susceptibility measurements indicated that **1** remained in a high-spin state between 1.8 and 300 K.

Keywords: Synthesis; Triazole; Crystal structure; Iron(II) complex

1. Introduction

Metal complexes with substituted 1,2,4-triazole ligands have attracted considerable attention in coordination chemistry due to their rich coordination modes and versatile properties [1–3]. Especially, iron(II) complexes of these ligands show intriguing spin-crossover (SCO) properties which can be applied in molecular electronics as information storage and switching materials [4–10]. Among them, mononuclear iron(II) complex, *trans*-$[Fe(ABPT)_2(NCS)_2]$ (ABPT = 4-amino-3,5-bis(2-pyridyl)-1,2,4-triazole), is an interesting example because it exhibited SCO properties associated with polymorphic behavior (red polymorph A, $T_{1/2} = 180$ K [11]; orange polymorph B, high-spin [12]; polymorph C, partial SCO at 86 K [13]; polymorph D, partial SCO at 162 K [13], and a long-lived photoinduced metastable state through NCS^- linkage isomerization accompanied with a SCO at 108 K [14]). It was also found that one pyridyl of ABPT was not coordinated in *trans*-$[Fe(ABPT)_2(NCS)_2]$; so, it is possible to replace a pyridyl by other aryl groups without changing the basic coordination of the ligand to the metal. Based on this, we recently synthesized an ABPT derivative, 4-amino-3-(*p*-chlorophenyl)-5-(2-pyridyl)-1,2,4-triazole (L′), and its iron(II) complex, *trans*-$[FeL'_2(NCS)_2][FeL'_2(CH_3OH)_2](NCS)_2$, which represented the first example of any mononuclear triazole-based octahedral complex with

*Corresponding author. Email: zhudr@njut.edu.cn

coexistence of molecules with both *trans*-coordinated NCS^- and *trans*-CH_3OH [15]. As a continuation of our investigation on asymmetrically substituted 1,2,4-triazoles [16–23], we present here the synthesis of another new ABPT derivative, 4-amino-3-(*p*-bromophenyl)-5-(2-pyridyl)-1,2,4-triazole (**L**), and its iron(II) complex, *trans*-$[FeL_2(NCS)_2]$ (**1**), and their crystal structure and spectroscopic properties.

2. Experimental

2.1. *Materials and measurements*

All chemicals used were of analytical grade. Solvents were purified by conventional methods. Melting points were determined using an X4 digital microscopic melting point apparatus and are uncorrected. C, H, N, and S elemental analyses were obtained with a Thermo Finnigan Flash 1112A elemental analyzer. IR spectra were recorded on a Nicolet Avatar 380 FT-IR instrument with KBr pellets from 4000 to 400 cm^{-1}. ^1H NMR spectra were measured on a Bruker AM 500 MHz spectrometer at ambient temperature in $CDCl_3$. Chemical shifts are reported in parts per million (ppm) downfield from TMS. Electrospray ionization mass spectra (ESI-MS) were recorded with an LCQ advantage MAX mass spectrometer, with MeOH as the mobile phase; the flow rate of the mobile phase was 0.2 $cm^3\,min^{-1}$. The spray voltage was 4 kV and the capillary voltage was 40 V. Magnetic susceptibility data for **1** were measured on a Quantum Design MPMS-7 SQUID magnetometer between 1.8 and 300 K under 2000 Oe of external field. Diamagnetic corrections were made with Pascal's constants.

2.2. *Synthesis of L*

The synthetic route for **L** is shown in scheme 1. 2-(*p*-Bromophenyl)-5-(2-pyridyl)-1,3,4-oxadiazole (**A**) was synthesized according to our reported method [23]. A solution of **A** (1.81 g, 6.0 mmol) and anhydrous hydrazine (2 mL, 63.0 mmol) in anhydrous EtOH (20 mL) was stirred at 120 °C for 60 h. The unreacted hydrazine was removed under reduced pressure, and the crude product was purified by crystallization from anhydrous EtOH to provide **L** as a white solid in 67.3% yield. Single crystals of **L**, suitable for X-ray diffraction, were obtained by slow evaporation of an anhydrous EtOH solution at ambient temperature. m.p. 222–224 °C. Anal. Calcd for $C_{13}H_{10}N_5Br$ (%): C, 49.39; H, 3.19; N, 22.15. Found (%): C, 49.21; H, 3.05; N, 22.03. IR (cm^{-1}): ν = 3426(m), 3221(m), 3137(m), 1643(m), 1590(m), 1566(m), 1476(s), 1462(s), 1074(s), 1053(s), 996(s), 964(m), 825(s), 785(s), 721(s), 690(m). ^1H NMR δ: 6.43 (br, 2H, NH_2), 7.39 (dd, J_1 = 5.2 Hz,

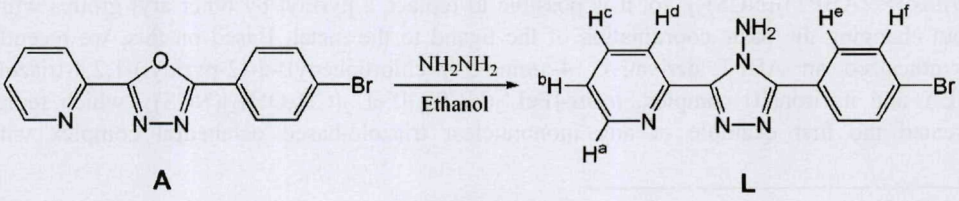

A L

Scheme 1. The synthetic route for **L**.

J_2 = 1.9 Hz, 1H, PyH[b]), 7.63 (d, J = 8.5 Hz, 2H, PhH[f]), 7.87–7.90 (m, 1H, PyH[c]), 8.15 (d, J = 8.5 Hz, 2H, PhH[e]), 8.36 (d, J = 8.0 Hz, 1H, PyH[d]), 8.64 (d, J = 4.6 Hz, 1H, PyH[a]) (figure S1). ESI-MS: m/z = 318.1.

2.3. *Synthesis of trans-[FeL$_2$(NCS)$_2$] (1)*

A solution of $FeSO_4 \cdot 7H_2O$ (0.2 mmol) in MeOH (2 mL) was added to a solution of KSCN (0.4 mmol) in anhydrous MeOH (2 mL). The mixture was stirred for 30 min, and then filtered. The K_2SO_4 precipitate was washed with 2 mL of anhydrous MeOH. The methanolic fractions containing $Fe(SCN)_2$ were combined and then poured into an MeOH solution of **L** (0.4 mmol). The resulting solution was stirred for 2 h during which an orange precipitate formed, which was isolated by filtration, washed with H_2O, and dried thoroughly in vacuo to give **1** (145 mg, 90.1%) as an orange powder. Orange single crystals suitable for X-ray diffraction were obtained by evaporation from MeOH solution under argon. Anal. Calcd for $C_{28}H_{20}Br_2FeN_{12}S_2$ (%): C, 41.81; H, 2.51; N, 20.90; S, 7.97. Found (%): C, 41.65; H, 2.33; N, 20.77; S, 7.82. FT-IR (cm^{-1}): 3354(s), 2078(vs), 1623(m), 1597(m), 1464(s), 1072(m), 1008(m), 831(w), 795(w). ESI-MS: m/z = 318.2, 746.2.

2.4. *Crystal structure determination*

Well-shaped single crystals of **L** and **1** were selected for X-ray diffraction studies. The unit cell parameters were determined and the intensity data were collected at 296(2) K on a Bruker SMART CCD diffractometer with a detector distance of 5 cm and frame exposure time of 8 s using graphite-monochromated Mo K_α (λ = 0.71073 Å) radiation. The structures were solved by direct methods and refined on F^2 by full-matrix least squares procedures using SHELXTL [24]. All nonhydrogen atoms were anisotropically refined. All hydrogens were generated geometrically and allowed to ride on their respective parent atoms, but not refined. Crystallographic data are summarized in table 1. Selected bond lengths and angles for **L** and **1** are listed in table 2.

3. Results and discussion

3.1. *Synthesis*

In contrast to the synthesis of L′, the asymmetrically substituted triazole **L** can be synthesized in one-pot reaction from 2-(*p*-bromophenyl)-5-(2-pyridyl)-1,3,4-oxadiazole in anhydrous hydrazine-EtOH solution. **L** reacted with an iron(II) salt and KSCN in a 2:1:2 molar ratio to form **1**, which is stable in air. The elemental analysis was satisfactory and consistent with a complex that contains one iron(II), two triazole ligands, and two NCS^-.

3.2. *Crystal structure of L*

A perspective of **L** with the atom-numbering scheme is shown in figure 1. X-ray structure analysis indicated that **L** crystallized in the triclinic space group *P-1* and its molecule structure is similar to L′ [15]. The molecule **L** is almost planar as the central 1,2,4-triazole ring is oriented at dihedral angles of 5.3(2)° and 4.0(2)° with respect to the pyridyl ring

Table 1. Crystal data and structure refinement parameters for **L** and **1**.

Compound	**L**	**1**
Empirical formula	$C_{13}H_{10}N_5Br$	$C_{28}H_{20}Br_2FeN_{12}S_2$
Formula weight	316.17	804.35
Crystal system	Triclinic	Monoclinic
Space group	*P-1*	$P2_1/n$
Unit cell dimensions (Å, °)		
a	5.952(2)	12.9208(10)
b	8.129(3)	9.4194(7)
c	12.908(5)	13.6099(11)
α	83.418(5)	90
β	88.002(4)	110.8460(10)
γ	88.015(5)	90
V (Å^3)	619.7(4)	1548.0(2)
Z	2	2
D_c (g cm^{-3})	1.694	1.726
μ (mm^{-1})	3.309	3.246
F (000)	316	800
Reflections collected	4400	10,652
Independent reflections	2156 [R_{int} = 0.0266]	2726 [R_{int} = 0.0280]
Reflections observed [$I > 2\sigma(I)$]	2299	2216
Data/restraints/parameters	2156/3/178	2726/3/211
Goodness-of-fit on F^2	1.052	1.031
Final R indices ($I > 2\sigma(I)$)	0.0288/0.0747	0.0346/0.0844
R indices (all data)	0.0350/0.0777	0.0460/0.0886
Largest difference peak and hole (eÅ^{-3})	0.253 and −0.297	1.010 and −0.794

Table 2. Selected bond distances (Å) and angles (°) for **L** and **1**.

L		**1**	
N1–C1	1.334(3)	Fe1–N1	2.233(3)
N1–C5	1.341(3)	Fe1–N2	2.169(2)
N2–C6	1.320(3)	Fe1–N6	2.115(3)
N3–C7	1.324(3)	S1–C14	1.635(4)
Br1–C11	1.899(2)	Br1–C11	1.908(3)
N2–N3	1.370(3)	N2–N3	1.379(3)
N4–N5	1.419(2)	N4–N5	1.413(4)
C6–N2–N3	108.20(16)	N1–Fe1–N2	74.18(9)
C6–C5–N1	117.98(18)	N1–Fe1–N6	88.29(10)
C7–N4–C6	106.60(16)	N2–Fe1–N6	87.64(10)
N5–N4–C7	126.06(16)	N6–C14–S1	178.1(3)
C10–C11–Br1	119.66(18)	Fe1–N6–C14	176.3(3)

and the *p*-bromophenyl ring, respectively. These dihedral angles are smaller than (8.6(3)° and 5.7(3)°) found in L′ [15]. The bond lengths and angles of **L** are within normal ranges and also similar to those found in the L′ and ABPT [15, 25]. However, there is a prominent difference in the crystal-packing interactions between **L** and L′. Intermolecular C4–H4A···N2^a hydrogen bonds link two **L** to form dimers, which are further connected by intermolecular N5–H5A···N2^b hydrogen bonds and an offset face-to-face $\pi\cdots\pi$ stacking interaction between pyridyl and triazole rings (centroid–centroid distance = 3.736(3) Å; dihedral angle = 5.3(2)°) to produce 1D chains along the *a* axis (figure 2 and table 3). In contrast, a face-to-face $\pi\cdots\pi$ stacking interaction only exists between the *p*-chlorophenyl and triazole rings in L′. In addition, there are two kinds of intramolecular hydrogen bonds in each **L** between the *p*-bromophenyl ring and amino group [C13–H13A···N5] and between the amino and pyridyl groups [N5–H5B···N1] (table 3).

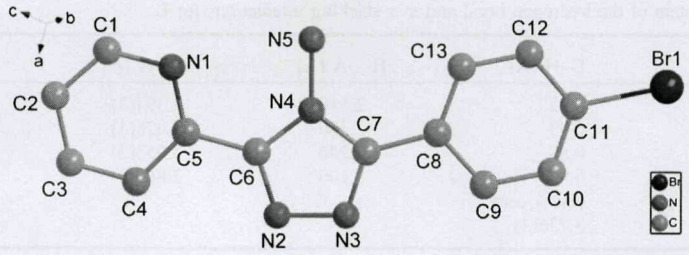

Figure 1. Projection of the structure of **L** with labeling system. Hydrogens are omitted for clarity.

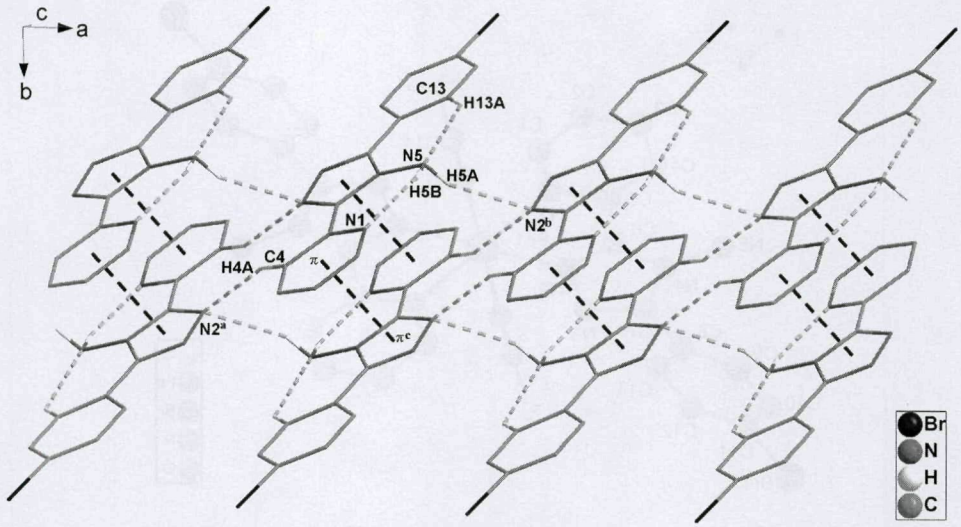

Figure 2. The crystal packing of **L** viewed along the *a* axis showing the hydrogen bonding and π–π stacking interactions.

3.3. *Crystal structure of 1*

Although **L** and L′ are similar, their iron(II) complexes, **1** and *trans*-$[FeL'_2(NCS)_2]$ $[FeL'_2(CH_3OH)_2](NCS)_2$, are totally different. Complex **1** crystallized in the monoclinic space group $P2_1/n$, and its structure with the atom numbering system is shown in figure 3. There is an inversion center at Fe. Fe is coordinated by four nitrogens from two **L** in the equatorial plane and two nitrogens from two NCS^- in the axial positions to form a distorted octahedron. All Fe–N bond lengths are inequivalent, and the N1–Fe–N2 bond angle deviates significantly from an ideal 90° due to the five-membered chelate ring (table 2). Each **L** coordinates to Fe(II) via N1 of the pyridyl ring and N2 of the triazole ring, similar to that observed in iron(II) complexes with ABPT [11, 12] and other substituted 1,2,4-triazoles [7, 15]. The average Fe–N bond length is 2.172(3) Å, within the typical range for a high-spin Fe(II)–N bond (2.051–2.248 Å) [6, 7, 26]. The spin-state assignment based on the Fe(II)–N bond distance is associated with octahedral distortion parameter (Σ), which is commonly used for quantification of the angular deviation of an octahedron from its ideal geometry [27]. A smaller Σ value is generally related with a stronger ligand field and, therefore, a low-spin state of the metal ion, while the opposite suggests a high-spin

Table 3. Parameters of the hydrogen bond and π–π stacking interactions for **L**.

D–H···A	D–H (Å)	H···A (Å)	D···A (Å)	∠D–H···A (°)
C4–H4A···N2[a]	0.93	2.510	3.394(3)	158
C13–H13A···N5	0.93	2.380	3.026(3)	126
N5–H5A···N2[b]	0.89	2.240	3.055(3)	151
N5–H5B···N1	0.89	2.100	2.864(3)	143
π···π interaction	cent···cent			dihedral angle
π (trz)···π (py)[c]	3.736(3)			5.3(2)

Symmetry codes: [a] $-1-x, 3-y, -z$; [b] $-x, 2-y, -z$; [c] $-x, 3-y, -z$.

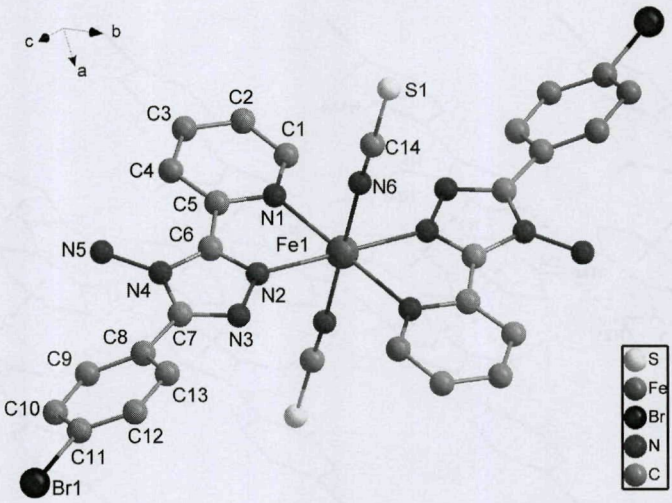

Figure 3. Projection of the structure of **1** with labeling system. Hydrogens are omitted for clarity.

state [26, 27]. In the present case, the Σ value is 79.44°, suggesting that Fe1 is in a high-spin state at 296 K (vide infra). The Fe–N_{py} distance is larger than that for Fe–N_{trz}, consistent with that found in analogous Fe(II) complexes [7, 15, 28–31]. The dihedral angle (5.7(3)°) between the pyridyl and triazole rings in **1** is slightly larger than that in free **L**, which is different from that observed in *trans*-[FeL′$_2$(NCS)$_2$][FeL′$_2$(CH$_3$OH)$_2$](NCS)$_2$, where the dihedral angles (4.2(2)° and 3.2(2)°) are smaller than that (8.6(3)°) in free L′ [15]. The *p*-bromophenyl-triazole twist angle (28.3(3)°) in **1** is much larger than that in free **L**. In addition, the co-ligand NCS^- and Fe1–N6–C14 angles are almost linear (N6–C14–S1 = 178.1(3)° and Fe1–N6–C14 = 176.3(3)°); the latter angle is larger than that (157.0(3)°) found in *trans*-[FeL′$_2$(NCS)$_2$][FeL′$_2$(CH$_3$OH)$_2$](NCS)$_2$ [15].

There are three kinds of intermolecular hydrogen bonds and one intramolecular hydrogen bond in the structure of **1** (table 4), linking the molecules of **1** into a 1D chain (figure 4). These hydrogen bond interactions are between the *p*-bromophenyl group and NCS^- anion [C9[d]–H9A[d]···S1, C13–H13A···S1[e]], the amino and *p*-bromophenyl groups [N5–H5B···Br1[d]], and the pyridyl and amino groups [C4–H4A···N5]. Moreover, the 1D chain is further stabilized by an offset face-to-face π···π[d] stacking interaction between pyridyl and *p*-bromophenyl ring (centroid–centroid distance = 3.864(3) Å; dihedral angle = 11.7(2)°).

Table 4. Parameters of the hydrogen bond and π–π stacking interactions for **1**.

D–H···A	D–H (Å)	H···A (Å)	D···A (Å)	∠D–H···A (°)
C4–H4A···N5	0.93	2.450	3.063(5)	123
C9[d]–H9A[d]···S1	0.93	2.810	3.575(4)	141
C13–H13A···S1[e]	0.93	2.860	3.627(4)	141
N5–H5B···Br1[d]	0.86	2.920	3.580(4)	135
$\pi\cdots\pi$ interaction	cent···cent			dihedral angle
π (*p*-bromophenyl)···π (py)[d]	3.864			11.7(2)

Symmetry codes: [d]1.5−*x*, 0.5+*y*, 0.5−*z*; [e]1.5−*x*, *y*−0.5, 0.5−*z*.

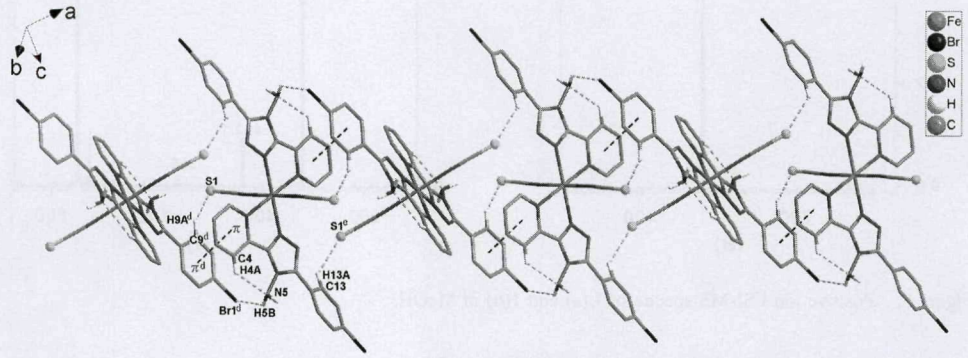

Figure 4. The 1D chain in **1** formed by hydrogen bonding and π–π stacking interactions.

3.4. *IR spectrum*

The IR spectrum of free **L** (figure S2) shows two medium-intensity bands at 1590 and 1566 cm^{-1} attributable to pyridyl ring vibrations. Upon coordination, the band of pyridine at larger cm^{-1} can shift about 15 wavenumbers [16]. So, in the spectrum of **1** (figure S3), the band at 1623 cm^{-1} can be assigned to coordinated pyridyl ring, showing that **L** binds via one pyridyl N. The strong band at 2078 cm^{-1} is assigned to C≡N stretching vibration of the *trans*-coordinated NCS^- groups [7, 15]. These features are in agreement with the results of X-ray crystallography. In addition, bands at 1074 and 1072 cm^{-1} are attributed to the C(Ph)–Br stretching vibrations in **L** and **1**, respectively [16]. Bands at 3221 and 3354 cm^{-1} are attributed to N–H stretching vibrations of the NH_2 in **L** and **1**, respectively [15].

3.5. *Electrospray ionization mass spectra (ESI-MS)*

The structures of **L** and **1** in solution were also studied by electrospray ionization mass spectra (ESI-MS) [32, 33]. Figure 5(a) displays the positive ESI mass spectrum of **L** in MeOH. The base peak at *m/z* 318.1 is the $[\mathbf{L}+H]^+$ ion. Figure 5(b) shows the positive ESI mass spectrum of **1** in MeOH. Two main peaks at *m/z* 318.2 and 746.2 are $[\mathbf{L}+H]^+$ and $[FeL_2(NCS)]^+$, respectively.

3.6. *Magnetic properties of 1*

The temperature dependence of the magnetic susceptibility of **1** was measured on a crystalline sample at an applied field of 2000 Oe. The χ_M and χ_M^{-1} *versus* *T* plots are

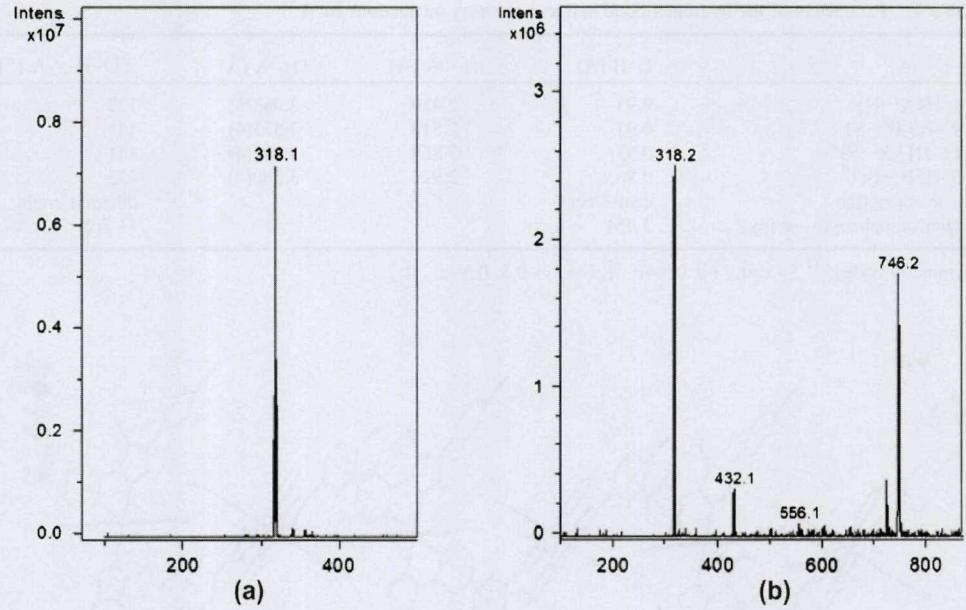

Figure 5. Positive ion ESI-MS spectra of **L**(a) and **1**(b) in MeOH.

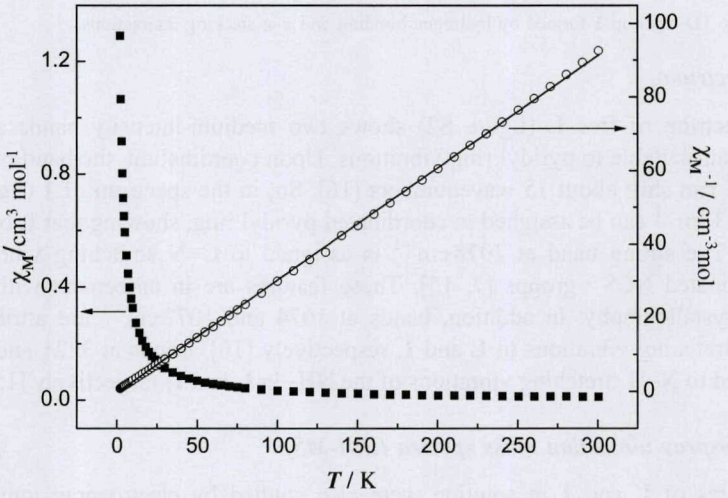

Figure 6. Plots of χ_M *vs.* T (■) and χ_M^{-1} *vs.* T (○) for **1**. Solid line represents the best linear fit.

shown in figure 6. The results reveal that **1** remained in a high-spin state between 1.8 and 300 K, which indicates the crystal-field splitting energy ($\Delta = 10Dq$) is lower than the electron pairing energy (P). This behavior is also consistent with the octahedral distortion parameter (Σ). In accordance with the Curie–Weiss law, $\chi_M = C/(T - \theta)$, the data for **1** show a good linear relationship between χ_M^{-1} and T with a Curie value of 3.28 and Weiss constant of −1.03 K, in agreement with that found in *trans*-[FeL′$_2$(NCS)$_2$] [15]. Although

both **L** and L′ are ABPT derivatives, their iron(II) complexes, **1** and *trans*-[FeL′$_2$(NCS)$_2$], are still high-spin species. On the contrary, *trans*-[Fe(ABPT)$_2$(NCS)$_2$] showed SCO properties. These results reveal that after one pyridyl of ABPT is replaced by *p*-bromophenyl or *p*-chlorophenyl, the ligand field strength resulting from **L** or L′ cannot be shifted to the region of SCO for their Fe(II) complexes with NCS^- as co-ligands.

4. Conclusions

A new asymmetrically substituted 1,2,4-triazole, 4-amino-3-(*p*-bromophenyl)-5-(2-pyridyl)-1,2,4-triazole (**L**), and its iron(II) complex, *trans*-[FeL$_2$(NCS)$_2$] (**1**), have been synthesized and characterized. Crystallographic studies revealed that **L** is planar and that **1** is a mononuclear distorted octahedral iron(II) complex with two *trans* NCS^-. Each **L** coordinates to Fe(II) via N1 of the pyridyl ring and N2 of the triazole ring. Complex **1** is a high-spin species from 1.8 to 300 K.

Supplementary material

The ^{1}H NMR spectra of **L** and IR spectra of **L** and **1**. Crystallographic data for the structures reported in this article have been deposited with the Cambridge Crystallographic Data Center as supplementary publication Nos. CCDC 916981 (**L**) and 916982 (**1**). Copies of the data can be obtained free of charge via www.ccdc.cam.ac.uk (or from the Cambridge Crystallographic Center, 12 Union Road, Cambridge CB21EZ, UK; Fax: +44 1223 336033; E-mail: deposit@ccdc.cam.ac.uk).

Acknowledgments

This work was funded by the National Nature Science Foundation of China (Nos. 20771059 and 21171093) and the State Key Laboratory of Materials-oriented Chemical Engineering (KL11-03).

References

[1] J.G. Haasnoot. *Coord. Chem. Rev.*, **200**, 131 (2000).
[2] M.H. Klingele, S. Brooker. *Coord. Chem. Rev.*, **241**, 119 (2003).
[3] J.A. Kitchen, S. Brooker. *Coord. Chem. Rev.*, **252**, 2072 (2008).
[4] O. Kahn, C.J. Martinez. *Science*, **279**, 44 (1998).
[5] D. Zhu, L. Qi, H. Cheng, X. Shen, W. Lu. *Prog. Chem.*, **21**, 1187 (2009).
[6] P.J. van Koningsbruggen. *Top. Curr. Chem.*, **233**, 123 (2004).
[7] D. Zhu, Y. Xu, Z. Yu, Z. Guo, H. Sang, T. Liu, X. You. *Chem. Mater.*, **14**, 838 (2002).
[8] J. Kröber, E. Codjovi, O. Kahn, F. Grolière, C. Jay. *J. Am. Chem. Soc.*, **115**, 9810 (1993).
[9] X. Bao, J.L. Liu, J.D. Leng, Z. Lin, M.L. Tong, M. Nihei, H. Oshio. *Chem. Eur. J.*, **16**, 7973 (2010).
[10] X. Bao, P.H. Guo, W. Liu, J. Tucek, W.X. Zhang, J.D. Leng, X.M. Chen, I. Gural'skiy, L. Salmon, A. Bousseksou, M.L. Tong. *Chem. Sci.*, **3**, 1629 (2012).
[11] N. Moliner, M.C. Muñoz, S. Letard, J.F. Letard, X. Solans, R. Burriel, M. Castro, O. Kahn, J.A. Real. *Inorg. Chim. Acta*, **291**, 279 (1999).
[12] A.B. Gaspar, M.C. Muñoz, N. Moliner, V. Ksenofontov, G. Levchenko, P. Gütlich, J.A. Real. *Monatsh. Chem.*, **134**, 285 (2003).
[13] C.F. Sheu, S.M. Chen, S.C. Wang, G.H. Lee, Y.H. Liu, Y. Wang. *Chem. Commun.*, **7512**, (2009).
[14] C.F. Sheu, C.H. Shih, K. Sugimoto, B.-M. Cheng, M. Takata, Y. Wang. *Chem. Commun.*, **48**, 5715 (2012).
[15] L. Wang, J.J. Jiang, L. Chen, X. Shen, D.R. Zhu. *Inorg. Chem. Commun.*, **28**, 104 (2013).

[16] W. Lu, D.R. Zhu, Y. Xu, H.M. Cheng, J. Zhao, X. Shen. *Struct. Chem.*, **21**, 237 (2010).
[17] J. Zhao, H.M. Cheng, G.P. Shen, Y. Xu, D.R. Zhu. *J. Coord. Chem.*, **64**, 942 (2011).
[18] G.P. Shen, J. Zhao, J.J. Jiang, Q. Liu, X. Shen, Y. Xu, D.R. Zhu, X.Q. Liu. *J. Mol. Struct.*, **1002**, 159 (2011).
[19] L. Chen, J. Zhao, G.P. Shen, X. Shen, Y. Xu, D.R. Zhu, J. Wang. *J. Coord. Chem.*, **64**, 3980 (2011).
[20] J. Zhao, W. Lu, L. Chen, X. Shen, Y. Xu, D.R. Zhu. *Chinese J. Inorg. Chem.*, **27**, 743 (2011).
[21] J. Zhao, G.P. Shen, Y. Zhang, X. Shen, D.R. Zhu. *J. Heterocycl. Chem.*, **49**, 1114 (2012).
[22] G.P. Shen, J. Zhao, L. Chen, F. Sun, X. Shen, D.R. Zhu, X.Q. Liu. *Chinese J. Inorg. Chem.*, **28**, 159 (2011).
[23] G.P. Shen, L. Qi, L. Wang, Y. Xu, J.J. Jiang, D.R. Zhu, X.Q. Liu, X. You. *Dalton Trans.*, **42**, 10144 (2013)
[24] G.M. Sheldrick. *Acta Crystallogr.*, **A64**, 112 (2008).
[25] M. Ramos Silva, J.A. Silva, N.D. Martins, A. Matos Beja, A.J.F.N. Sobral. *Acta Crystallogr.*, **E64**, o1762 (2008).
[26] P. Guionneau, M. Marchivie, G. Bravic, J.F. Létard, D. Chasseau. *Top. Curr. Chem.*, **234**, 97 (2004).
[27] P. Guionneau, M. Marchivie, G. Bravic, J.F. Létard, D. Chasseau. *J. Mater. Chem.*, **12**, 2546 (2002).
[28] L. Zhang, G.C. Xu, H.B. Zhang, T. Zhang, Z.M. Wang, M. Yuan, S. Gao. *Chem. Commun.*, **46**, 2554 (2010).
[29] J.A. Kitchen, G.N. Jameson, J.L. Tallon, S. Brooker. *Chem. Commun.*, **46**, 3200 (2010).
[30] J. Klingele, D. Kaase, M.H. Klingele, J. Lach, S. Demeshko. *Dalton Trans.*, **39**, 1689 (2010).
[31] B. Li, R.J. Wei, J. Tao, R.B. Huang, L.S. Zheng, Z.P. Zheng. *J. Am. Chem. Soc.*, **132**, 1558 (2010).
[32] S.R. Wilson, A. Yasmin, Y. Wu. *J. Org. Chem.*, **57**, 6941 (1992).
[33] R. Arakawa, T. Matsuo, H. Ito, I. Katakuse, K. Nozaki, T. Ohno, M.-A. Haga. *J. Mass Spectrom.*, **29**, 289 (1994).